Adsorption (2014) 20:109–119
DOI 10.1007/s10450-013-9553-0

On-line optimizing control of the intermittent simulated moving bed process

Shigeharu Katsuo · Cristian Grossmann · Manfred Morari · Marco Mazzotti

Received: 20 January 2013 / Accepted: 31 May 2013 / Published online: 19 June 2013

Abstract The I-SMB process is one of the modifications to the standard SMB process that has been demonstrated both theoretically and experimentally to exhibit rather competitive performance (Katsuo and Mazzotti in J Chromatogr A 1217:1354, 2010a, 3067, 2010b; Katsuo et al. in J Chromatogr A 1218:9345, 2011). This work aims at showing that also the I-SMB process can be controlled and optimized by using the optimizing on-line controller developed at ETH Zurich for the standard SMB process (Erdem et al. in Ind Eng Chem Res 43:405, 2004a, 3895, 2004b; Grossmann et al. in Adsorption 14:423, 2008, AIChE J 54:1942008). This is achieved by using a virtual I-SMB unit based on a detailed model of the process; past experience with the on-line controller shows that the controller's behavior on a virtual platform is essentially the same as in laboratory experiments.

Keywords Simulated moving bed chromatography · I-SMB · Separation of enantiomers · Tröger's base · On-line optimizing control

S. Katsuo · M. Mazzotti (✉)
Institute of Process Engineering, ETH Zurich, Sonneggstrasse 3, 8092 Zurich, Switzerland
e-mail: marco.mazzotti@ipe.mavt.ethz.ch

Present Address:
S. Katsuo
Mitsubishi Chemical Group, Science and Technology Research Center Inc, 1000, Kamoshida-cho, Aoba-ku, Yokohama 227-8502, Japan

C. Grossmann · M. Morari
Automatic Control Laboratory, ETH Zurich, Physikstrasse 3, 8092 Zurich, Switzerland

List of symbols

$a_{i,k}$, $b_{i,k}$	Parameters in bi-Langmuir isotherm for component i
c_i	Fluid phase concentration of component i
c_F^T	Total feed concentration
c_{P}, i	Concentration of component i at port P
$\bar{c}_{P,i}$	Average concentration of of component i at port P
D_i	Axial dispersion coefficient of component i
H_i	Henry's constant of component i
$k_{s,i}a_v$	Product of mass transfer coefficient and specific surface of component i
L	Column length
m_j	Flow rate ratio in section j of conventional SMB and I-SMB
n_i^*	Adsorbed phase concentration of component i in equilibrium with the mobile phase
n_j	Number of the columns in section j
Pr	Productivity
ΔP	Pressure drop
Q_j	Volumetric flow rate in section j
$\hat{Q}_j$	Average volumetric flow rate in section j
Q_P	Volumetric flow rate at port P
s_k	Slack variables
S	Column cross-section
SC	Dimensionless solvent consumption
t	Time
t^*	Switch time
u	Superficial velocity
V	Column volume
X_i	Product purity
Y_i	Recovery of component i

Greek letters

α	step ratio of I-SMB
ε^*	Overall bed void fraction
ε_b	Inter particle void fraction

λ Weights in objective function
ϕ Pressure drop factor

Subscripts and superscripts

A	Component A
B	Component B
i	Component index
j	Section index
SMB	Conventional SMB
I-SMB	I-SMB

1 Introduction

This work deals with the the Intermittent Simulated Moving Bed (I-SMB) process, which has been described, analyzed theoretically, and demonstrated experimentally in a series of earlier papers (Katsuo and Mazzotti 2010a, b; Katsuo et al. 2011). I-SMB chromatography is an implementation of continuous multi-column chromatography, i.e. a family of processes that are particularly attractive for applications in the fine chemical and pharmaceutical industries, e.g. for the separation of the enantiomers of chiral compounds, and include the classical Simulated Moving Bed process as well as a number of modifications thereof (Rajendran et al. 2009; Ludemann-Hombourger et al. 2000; Schramm et al. 2003; Zhang et al. 2003; Keßler et al. 2008). A distinct feature of the I-SMB process is that it achieves high productivity at high purity even when only four columns are used (Katsuo and Mazzotti 2010b; Katsuo et al. 2011), i.e. something that is not possible in the case not only of the standard SMB process but also of the other SMB modifications mentioned above.

There exist well established theoretical tools to handle the complexity of multicolumn continuous chromatographic processes and to optimize their performance, namely both simplified and detailed SMB models that based on an accurate characterization of the system properties, particularly of the competitive adsorption isotherm of the species to be separated, allow predicting the SMB performance under different operating conditions. Using such models, particularly the simplified ones based on the so called equilibrium theory of chromatography, it is possible to derive simple and effective criteria for the design and optimization of the standard SMB, i.e. the so called "triangle theory" (Mazzotti et al. 1997; Mazzotti 2006; Rajendran et al. 2009). Some of these simplified criteria can be extended to some of the SMB-like processes, whereas it is another distinct feature of the I-SMB process that "triangle theory" can be applied to its design and optimization in a straightforward manner (Katsuo and Mazzotti 2010a, b; Katsuo et al. 2011).

Another approach towards handling the SMB complexity is that of exploiting process control as a way to tune operating conditions in order to optimize a specified objective function, typically productivity or recovery or a combination thereof, under certain process constraints, typically the fulfillment of product specifications given in terms of product purity (Rajendran et al. 2009). The SMB optimizing controller, which was developed at ETH Zurich and successfully tested both on a virtual plant and on a real plant for a number of different separations, is based on repetitive model predicted control and uses a very simplistic model of the SMB unit, i.e. based on a very few parameters that are easy to measure, whose prediction is continuously corrected using feedback information about the composition of the product streams and a Kalman filter (Erdem et al. 2004a, b; Grossmann et al. 2008a, b).

The objective of this work is that of bringing together these two lines of research and of demonstrating the successful applicability of the ETH Zurich SMB optimizing controller "as is" to the I-SMB process. In principle a SMB controller developed for the standard SMB process cannot directly be used for a modified SMB process, unless the underlying model is properly adapted. Why should this work then? There are two compelling reasons that should be clear to the reader familiar with our work on SMB control and on I-SMB, whose key information are summarized for the sake of clarity in the next section of this paper.

On the one hand, the model, on which our controller is based, is a linearized SMB model where adsorption of all species follows linear isotherms, i.e. its characterization is effortless, and the process dynamics is rendered in terms of a high level cycle-to-cycle evolution (where a cycle is the time corresponding to a number of port switches equal to the number of columns in the unit) (Erdem et al. 2004). The strength of the controller is that despite the model simplifications it is able to cope not only with model-plant mismatch due to poor estimation of the Henry's constants (because of several possible reasons) but also with strong nonlinearities in the adsorption isotherms that are not at all incorporated in the controller's model. It is also worth mentioning that the controller performance has consistently been the same when applied to both a virtual plant, i.e. a plant simulated by a detailed process model, and to a real plant, i.e. an experimental set-up, the only differences being due to the obviously different accuracy of the feedback information. This is why a big effort has been devoted to the realization of an online monitoring system of the product compositions, particularly in the case of application to chiral substances (Langel et al. 2009; Grossmann et al. 2013).

On the other hand, we argue that, while the dynamics of the two processes during a switch interval, of duration t^*, is rather different, the cycle-to-cycle dynamics of the I-SMB process is very similar to that of the standard SMB process.

This is demonstrated by the observation that, since the cycle-to-cycle dynamics controls the cyclic steady state of the two processes, then "triangle theory", which is developed for a standard SMB and is based on a steady state true moving bed approximation of the SMB (Mazzotti et al. 1997), applies also to the I-SMB process as shown earlier (Katsuo and Mazzotti 2010a, b; Katsuo et al. 2011). We assume that the differences between SMB and I-SMB, which are of course important in determining the attractiveness of I-SMB with respect to standard SMB, can be dealt with by the feedback mechanism implemented in the controller. This is exactly what we want to demonstrate with the analysis and the results presented in the following.

2 Cycle to cycle optimizing control of the I-SMB process

2.1 The I-SMB process

In a standard SMB unit the continuous countercurrent movement of fluid and adsorbed phases is simulated by periodically switching, every t^* time units, in the same direction of the fluid flow the inlet and outlet ports to a set of identical chromatographic columns. The typical SMB unit consists of four sections, which are divided by two inlets and two outlets in such a way that the feed and the mobile phase (desorbent) are introduced between Sects. 2 and 3 and between Sects. 4 and 1, respectively, while the extract (consisting mainly of the more retained species A) is collected between Sects. 1 and 2 and the raffinate (containing mostly the less retained component B) is withdrawn between Sects. 3 and 4. The outlet of Sect. 4 can be recycled to Sect. 1 directly (closed-loop configuration) or collected and possibly recycled off-line (open-loop configuration).

The I-SMB process in turn is operated in two different modes during the two sub-intervals in which one switch period t^* is subdivided. During the first step I, of duration αt^* $(0 < \alpha < 1)$, the unit is operated as a three-section standard SMB, where as usual the feed and the desorbent are introduced, the extract and the raffinate are collected, but there is no flow in Sect. 4. During the second step II, of duration βt^* (with $\beta = 1 - \alpha$), the inlets and outlets ports are shut off and the fluid phase is circulated through all four sections of the unit in order to adjust the relative position of the concentration profiles with respect to the inlet and outlet ports (Katsuo and Mazzotti 2010a).

2.2 Control approach

The optimizing SMB controller developed at ETH Zurich is based on a very simple model of the unit and requires minimal tuning (Erdem et al. 2004a, b; Grossmann et al. 2008a, b). The optimizing SMB controller has been demonstrated effective through simulations using a virtual SMB unit for systems subject to linear and nonlinear isotherms (Abel et al. 2004; Erdem et al. 2004; Grossmann et al. 2008b) from the experimental point of view, the controller has been successfully applied to a number of systems, including chiral separations (Amanullah et al. 2007; Langel et al. 2009).

In the optimizing control system for the standard SMB process, the control variables are the flow rates Q_j^{SMB} $(j = 1, 2, 3, 4)$ in the four sections of the SMB unit, which are selected and updated by the controller only once every SMB cycle, and kept constant during one entire cycle. Such a choice is determined by the controller so as to optimize a specified objective function (typically defined so as to maximize productivity and to minimize solvent consumption) under a set of constraints, i.e. by maintaining the required product specifications, i.e. the product purities, and by satisfying certain process constraints, e.g. a given maximum total pressure drop. This is achieved by dynamically solving the optimization problem using the simplified SMB model and feedback information, namely the average outlet compositions over one entire cycle (Grossmann et al. 2008), and by applying Repetitive Model Predictive Control (RMPC), details of which can be found elsewhere (Erdem et al. 2004; Grossmann et al. 2008). Note that the SMB process model used in RMPC is a very simple, locally linearized model, which requires only the Henry's constants of the species to be separated and the average value of the column void fraction. Even in case of nonlinear separation, i.e. where the mixture to be separated is subject to a nonlinear adsorption isotherm, the controller can successfully find the optimal operating conditions without any knowledge of the system nonlinearity (Langel et al. 2009). This is made possible by the fact that the predictions issued by the simplistic model (using linear isotherms) are continuously corrected using feedback information from the plant about the composition of the product streams (depending on the nonlinear isotherm to which the real system is subjected) and a Kalman filter; the efficacy of this approach has been discussed and demonstrated in a number of previous papers (Erdem et al. 2004a, b; Grossmann et al. 2008a, b).

2.3 Equivalence between I-SMB and standard SMB

Consider two species A and B subject to a linear adsorption isotherm:

$$n_i^* = H_i c_i \quad (i = \mathrm{A}, \mathrm{B}), \tag{1}$$

with $H_{\mathrm{A}} > H_{\mathrm{B}}$, where c_i and n_i are the fluid phase and the adsorbed phase concentration of the ith component, respectively, H_i is its Henry's constant, and the asterisk identifies the adsorbed phase concentration in equilibrium with the fluid phase.

For the standard SMB process, the operating conditions can be determined in terms of the flow rate ratio in each SMB section, i.e.:

$$m_j^{\mathrm{SMB}} \equiv \frac{Q_j^{\mathrm{SMB}} t^* - V\epsilon^*}{V(1-\epsilon^*)} \quad (j = 1, \ , 4), \tag{2}$$

where V is the column volume and ϵ^* is the column overall void fraction.

In the frame of Triangle Theory (Mazzotti et al. 1997), it can be shown that the following criteria (inequalities) guarantee attainment of complete separation:

$$m_4 \le H_{\mathrm{B}} \le m_2 < m_3 \le H_{\mathrm{A}} \le m_1. \tag{3}$$

Earlier we have shown that the complete separation constraints for the I-SMB process are given exactly by the same form (Eq. 3) provided that they are applied to the following average flow rate ratios (Katsuo and Mazzotti 2010a):

$$m_j^{\mathrm{I-SMB}} \equiv \frac{\hat{Q}_j^{\mathrm{I-SMB}} t^* - V\epsilon^*}{V(1-\epsilon^*)}, \tag{4}$$

which are defined in terms of the following average flow rates in each I-SMB section: $\hat{Q}_j^{\mathrm{I-SMB}} \equiv \alpha Q_j^{\mathrm{I-SMB}} + \beta Q_4^{\mathrm{I-SMB}} (j = 1, 2, 3); \hat{Q}_4^{\mathrm{I-SMB}} \equiv \beta Q_4^{\mathrm{I-SMB}}$. Here α and β are the fraction of duration of the first and second sub-interval, respectively, of the time period t^* between two port switches, with $\beta = 1 - \alpha$.

According to the minimum switch time design, when applying the same flow rate ratio values and the same pressure drop constraint $\Delta P_{\mathrm{total}}$ to both an I-SMB and a standard SMB unit with the same column configuration, i.e. $m_j^{\mathrm{SMB}} = \hat{m}_j^{\mathrm{I-SMB}}$ and $\Delta P_{\mathrm{total}}^{\mathrm{SMB}} = \Delta P_{\mathrm{total}}^{\mathrm{I-SMB}}$, the switch time of both processes is given as follows and the same throughput can be achieved (Katsuo and Mazzotti 2010a, b; Katsuo et al. 2011):

$$t_{\mathrm{SMB}}^* = t_{\mathrm{I-SMB}}^* = \frac{\phi L^2}{\Delta P_{\mathrm{total}}} \sum_{j=1}^{4} n_j \left(m_j (1-\epsilon^*) + \epsilon^* \right), \tag{5}$$

where L is the column length, and ϕ is the proportionality factor in Darcy's law, i.e. the relationship $\Delta P / L = \phi Q / S$ (S is the column cross-sectional area). Therefore a standard SMB process operated under certain specific conditions has a unique equivalent I-SMB process, whose operating conditions can be calculated as follows:

- assigned SMB operating conditions

$$t_{\mathrm{SMB}}^*, m_j^{\mathrm{SMB}} \quad (j = 1, \ldots, 4). \tag{6}$$

- equivalence between I-SMB and standard SMB

$$t^* = t_{\mathrm{I-SMB}}^* = t_{\mathrm{SMB}}^*, \quad m_j = m_j^{\mathrm{I-SMB}} = m_j^{\mathrm{SMB}} \quad (j = 1, \ldots, 4). \tag{7}$$

- equivalent I-SMB operating conditions

$$\begin{cases} \alpha = \dfrac{\sum_{j=1}^{3} n_j \left(m_j - m_4 \right)(1-\epsilon^*)}{\sum_{j=1}^{4} n_j \left(m_j (1-\epsilon^*) + \epsilon^* \right)}, \quad \beta = 1 - \alpha, \\ Q_j^{\mathrm{I-SMB}} = \dfrac{(m_j - m_4) V (1-\epsilon^*)}{\alpha t^*} \quad (j = 1, 2, 3), \\ Q_4^{\mathrm{I-SMB}} = \dfrac{m_4 V (1-\epsilon^*) + V\epsilon^*}{\beta t^*}. \end{cases} \tag{8}$$

2.4 Optimizing I-SMB controller

The relationships of Eqs. 6, 7 and 8 make it possible to apply the existing standard SMB controller to the I-SMB unit. Figure 1 shows the scheme of the I-SMB optimizing controller, which is an extension of the standard SMB controller. In fact the only difference is that the operating conditions determined by the controller, which refer to a standard SMB unit, are converted into I-SMB operating conditions by the newly added "I-SMB converter". This is done using Eq. 8 that allow calculating the four flow rates $Q_j^{\mathrm{I-SMB}}$ and the duration of the first sub-interval $\alpha\ t^*$. Note that the switch time t^* is fixed, and is not modified by the controller.

It is worth noting that the I-SMB process and the standard SMB process are rather different in terms of switching sequence and of dynamics during a switch interval, of

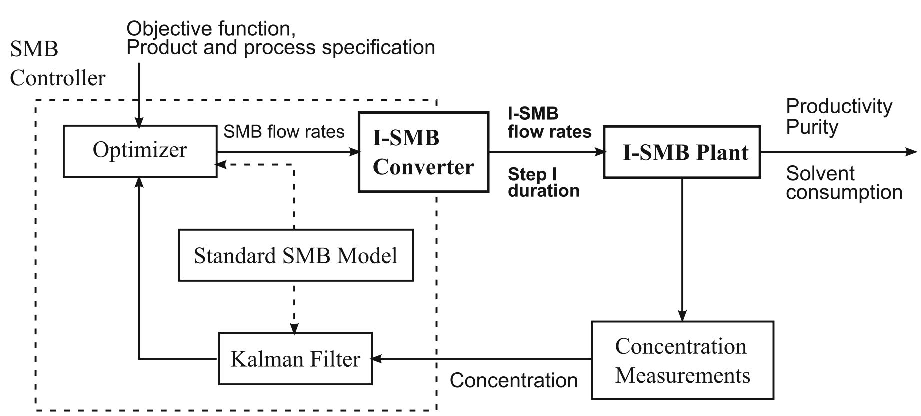

Fig. 1 'Cycle to cycle' control scheme modified for the I-SMB process

duration t^*; this is the very reason of the I-SMB's special features and better performance with respect to the standard SMB (Katsuo and Mazzotti 2010a). Nevertheless, we expect that the controller presented here should work also for the I-SMB process, because the two processes have a very similar high level cycle-to-cycle dynamics, and both processes can be analyzed and designed in the operating space, i.e. the space spanned by the four flow rate ratios, and because of how the SMB controller is flexible and powerful.

2.5 Formulation of the constrained optimization problem

The optimizing controller calculates the operating conditions, which make the product streams (extract and raffinate) fulfill the process specification and maximize the performance of the unit in terms of a specified objective function, while satisfying all required process constraints. The optimization problem, including the constraints and the objective function, is formulated as a Linear Programming (LP) problem as described briefly in the following (see previous papers for details (Grossmann et al. 2008)).

2.5.1 *Constraints*

The purity of each product stream, i.e. the quantity of interest in most cases on which process specifications are typically based, is defined as:

$$X_A = \frac{\bar{c}_{E,A}}{\bar{c}_{E,A} + \bar{c}_{E,B}}, \quad X_B = \frac{\bar{c}_{R,B}}{\bar{c}_{R,A} + \bar{c}_{R,B}}. \tag{9}$$

where $\bar{c}_{E,i}$ and $\bar{c}_{R,i}$ are the average concentrations of each component in the extract and the raffinate stream, respectively. In order to incorporate effectively the constraints into the LP problem, the purity specifications are linearized and given as the following inequalities, where the slack variables s_k are introduced; they will be kept small by the optimizer by including them into the objective function (see below):

$$\begin{aligned} X_A &\geq X_{A,\min} - s_1 \quad s_1 \geq 0, \\ X_B &\geq X_{B,\min} - s_2 \quad s_2 \geq 0. \end{aligned} \tag{10}$$

Additional process constraints arise because of practical considerations about the I-SMB equipment. In this work the following constraints are applied, so as to limit pressure drop and flow rate changes:

$$\Delta P_{\text{total}} \leq P_{\max}, \tag{11}$$

$$|\Delta \mathbf{Q}| \leq \mathbf{s}_3. \tag{12}$$

In these equations $\Delta\mathbf{Q} = [\Delta Q_1, \Delta Q_2, \Delta Q_3, \Delta Q_4]^T$ is the change of the flow rate in section j from one cycle to the next, and $\mathbf{s}_3$ is a vector consisting of the corresponding slack variables. In the case of the I-SMB process the following additional constraint on the average flow rate ratios has to be fulfilled in order to make sure that the flow rates $Q_j^{\text{I-SMB}}$ ($j = 1, 2, 3$) be positive:

$$m_j \geq m_4 \quad (j = 1, 2, 3), \tag{13}$$

2.5.2 *Objective function*

The indicators of performance associated to the process rentability and to its costs are the productivity Pr and the solvent consumption SC, which are defined for the two processes as:

$$Pr^{\text{SMB}} = \frac{Q_F(Y_A c_{F,A} + Y_B c_{F,B})}{\sum n_j V}, \tag{14}$$

$$Pr^{\text{I-SMB}} = \frac{\alpha Q_F(Y_A c_{F,A} + Y_B c_{F,B})}{\sum n_j V}, \tag{15}$$

$$SC = \frac{(Q_D + Q_F)(c_{F,A} + c_{F,B})}{Q_F(Y_A c_{F,A} + Y_B c_{F,B})}. \tag{16}$$

where $Y_A = Q_E c_{E,A}/Q_F c_{F,A}$ and $Y_B = Q_R c_{R,B}/Q_F c_{F,B}$ are the yield of the species collected in the extract and raffinate, respectively. Note that the indicators above are defined in terms of the feed concentrations, which are independent of the operating conditions and of the separation's efficacy; this is legitimate because through the constraints on the optimization problem the process is guaranteed to fulfill the process specifications.

For the sake of simplicity in this study, the switch time t^* and the flow rate ratios in Sect. 1 and 4 (m_1 and m_4) are kept constant, which implies that the values of Q_1 and Q_4 are also constant in both standard SMB and I-SMB operations. Moreover, an equimolar feed mixture, e.g. of chiral compounds, i.e. $c_{F,A} = c_{F,B} = c_F^T/2$, is considered and the specified purity of extract and raffinate is the same, i.e. $X_{A,\min} = X_{B,\min} = X_{\min}$. Under these provisions and accounting for the overall mass-balances at cyclic-steady state taking into account the conditions on the feed concentration of each component Eqs. 14 to 16 can be recast as:

$$Pr^{\text{SMB}} = \frac{XQ_F c_F^T}{2\sum n_j V}, \quad Pr^{\text{I-SMB}} = \frac{\alpha X Q_F c_F^T}{2\sum n_j V}, \tag{17}$$

$$SC = \frac{2(Q_D + Q_F)}{XQ_F}, \tag{18}$$

or in terms of the flow rate ratios as:

$$Pr^{\text{SMB,I-SMB}} = \frac{Xc_F^T(m_3 - m_2)(1 - \epsilon^*)}{2\sum n_j t^*}, \tag{19}$$

$$SC = \frac{2(m_1 - m_4 + m_3 - m_2)}{X(m_3 - m_2)}, \tag{20}$$

Since from Eqs. 17 and 18 it is obvious that the performance of the unit can be improved by increasing the feed flow rate Q_F and by decreasing the desorbent flow rate Q_D, minimizing the following objective function is equivalent to maximizing rentability and minimizing costs, while at the same fulfilling the constraints by minimizing the value of the slack variables. Thus the constrained optimization problem can be defined as follows:

$$\min_{Q_2,Q_3,\mathbf{s}}[\lambda_D Q_D - \lambda_F Q_F + \boldsymbol{\lambda}_s \cdot \mathbf{s}], \tag{21}$$

where the weights λ_D, λ_F and $\boldsymbol{\lambda}_s$ reflect the relative importance given to the different terms of the cost function, and **s** is the vector consisting of the slack variables. Based on previous experience (Grossmann et al. 2009), the following values of the weights have been utilized in the simulations reported in this work: $\lambda_D = 5, \lambda_F = 30, \boldsymbol{\lambda}_s = [\lambda_1, \lambda_2, \boldsymbol{\lambda}_3]$ with $\boldsymbol{\lambda}_3 = [1000, 1500, 1500, 1000]$ always, and the following values of the other two parameters depending on the process and the feed concentration considered: for SMB and I-SMB 1-2-2-1, $\lambda_1 = \lambda_2 = 1$; for SMB 1-1-1-1, $\lambda_1 = \lambda_2 = 1$ at 1 g/L feed concentration, and $\lambda_1 = \lambda_2 = 1.25$ at 15 g/L feed concentration; and finally for I-SMB 1-1-1-1, $\lambda_1 = \lambda_2 = 1.25$ at 1 g/L feed concentration, and $\lambda_1 = \lambda_2 = 2$ at 15 g/L feed concentration. The problem defined above is solved with the help of the LP solver named SeDuMi, which has been developed at Computational Optimization Research in Lehigh, VA, USA (COR@L) (Sturm et al. 1999).

3 Results and discussion

In this section the on-line optimizing control of the I-SMB process is applied and its efficacy is demonstrated through simulations using a virtual plant, and the results are analyzed in the frame of Triangle Theory.

3.1 Virtual plant

Let us consider the separation of the racemic mixture of the Tröger's base enantiomers, (±)-2,8-dimethyl-6H,12H-5,11-methanodibenzo[b,f] [1,5]diazocine, in ethanol (mobile phase) on the stationary phase Chiralpak AD. Such a system was studied elsewhere (Katsuo and Mazzotti 2010; Katsuo et al. 2011), and the competitive adsorption isotherms of the two enantiomers was found to be a bi-Langmuir adsorption isotherm:

$$n_i^* = \frac{a_{i,1}c_i}{1 + b_{A,1}c_A + b_{B,1}c_B} + \frac{a_{i,2}c_i}{1 + b_{A,2}c_A + b_{B,2}c_B} \quad (i = A, B). \tag{22}$$

Both the I-SMB and the standard SMB separation of the two enantiomers were carried out experimentally.

Table 1 Column and system parameters (Katsuo and Mazzotti 2010b)

Column		
S (cm^2)	0.166	
L (cm)	15	
$\epsilon^*[-]$	0.68	
ΔP_{max} (bar)[a]	40	
System Characteristics	Component	
	A	B
Isotherm	Bi-Langmuir	
$a_{i,1}$ (−)	3.99	1.56
$b_{i,1}$ (L/g)	0.0107	0.0132
$a_{i,2}$ (−)	0.986	0.304
$b_{i,2}$ (L/g)	0.601	0.136
$k_{s,i}a_v$ (1/sec)[b]	1.81	2.96
$\epsilon_b D_i/u$ (m)[c]	3.01×10^{-4}	
ϕ (bar min/cm^2)[d]	0.1	

[a] Maximum allowable pressure drop of the column

[b] Product of mass transfer coefficient and specific surface

[c] Coefficient to determine the dispersion coefficient, where ϵ_b is bed void fraction and u is superficial velocity

[d] Proportionality coefficient in Darcy's law, $\Delta P/L = \phi Q/S$

The virtual plant considered here consists of four columns in the 1-1-1-1 configuration or of six columns in the 1-2-2-1 configuration and is operated in two different modes, i.e. I-SMB and standard SMB, thus giving four different operations to be considered and compared. The multi-column chromatographic detailed model used in the simulation is the same reported in Table 1 of an earlier paper (Katsuo et al. 2011). The corresponding equations are not reported here for the sake of brevity. All parameters of the model and the column characteristics are given in Table 1. Note that, although the simulations reported here are carried out for this specific set of parameters, our experience with both simulations and experiments indicates that the controller's performance is rather insensitive to the parameters' values, e.g. those characterizing the column efficiency. In Table 2, the information supplied to the controller is reported. It is worth noting that as far as the adsorption isotherms are concerned the controller knows only the Henry's constants of the two species, which in the case of a bi-Langmuir isotherm are $H_i = a_{i,1} + a_{i,2}$ (i = A,B).

3.2 Complete separation conditions

The theoretical shape, size and position of the complete separation region in the operating parameter space, particularly in the (m_2,m_3) plane, for an I-SMB as compared to that of a standard SMB process was studied in our previous

Table 2 Parameters for the on-line optimizing control

Geometric conditions	Configuration Column geometry	1-2-2-1 S, L, ϵ^*	1-1-1-1
Henry constants	H_A	4.976	
	H_B	1.864	
Constraints	$P_{total,max}$ [bar]	40.0	
	$X_{A,min}$ [−]	0.999	
	$X_{B,min}$ [−]	0.999	
Operating conditions	Fixed t^* [min]	6.3 4.2	
	Fixed (m_1, m_4)	(5.971, 1.222)	
	Initial (m_2, m_3)	(1.614, 5.226)	

papers on I-SMB. In the case of a linear isotherm it was shown rigorously that the same criteria as given by Eqs. 3 apply to both standard SMB and I-SMB, hence the same complete separation region can be drawn in the operating parameter space (Katsuo et al. 2010).

In the case where the mixture to be separated is subject to a nonlinear isotherm of the Langmuir or by-Langmuir type and a standard SMB process is considered in the frame of the Triangle Theory there is a procedure to obtain the relevant criteria on the flow rate ratios, which depend on adsorption isotherm parameters and feed composition, but not on the unit configuration (Mazzotti et al. 1997; Gentilini et al. 1998). Figure 1 of a previous paper (Katsuo et al. 2011) considers the model system presented in Sect. 1 and shows the complete separation regions calculated for the linear isotherm and for the bi-Langmuir isotherm at different overall concentration of the racemic mixture of the Tröger's base enantiomers, i.e. 1, 5, 10 and 15 g/L.; in the figures presented and discussed below expanded parts of these regions will be drawn. The upper bound for m_4 is calculated for the m_2 and m_3 values corresponding to the tip of the complete separation region. Note that all the simulations presented below have been carried with the same values of m_1 and m_4 (see Table 2); these values of m_1 and m_4 guarantee the solid and mobile phase regeneration in Sects. 1 and 4 during the SMB operation. When considering Eqs. 19 and 20 in the case where the values of m_1 and m_4 are fixed, it is rather obvious that the tip of the complete separation region (triangle), where the difference $m_3 - m_2$ is the largest, leads to the highest productivity and the lowest solvent consumption whilst achieving complete separation.

The effect of the SMB unit configuration, i.e. the number of columns and their distribution in the four different sections, can be analyzed using a detailed model of the multicolumn process, and making a parametric analysis of the separation performances for different points in the operating parameter space. By doing so one obtains the actual region in the operating parameter space where the complete separation can be achieved, i.e. the *real* complete separation region. This may in general be smaller than the *ideal* complete separation region predicted under the simplifying assumptions (no axial dispersion and no mass transfer resistance) applied within Triangle Theory. It was shown that in the case of the standard SMB process in the 1-2-2-1 configuration at any feed concentration the *real* complete separation region calculated for the model system above is almost identical to the *ideal* one, whereas the *real* complete separation region for the 1-1-1-1 configuration is much smaller (Katsuo and Mazzotti 2010b; Katsuo et al. 2011).

The approach based on the detailed simulations must be applied also to the I-SMB process under nonlinear chromatographic conditions, since in this case the Triangle Theory cannot be directly extended. We could conclude that for both the 1-2-2-1 and the 1-1-1-1 I-SMB processes the *real* complete separation region and the *ideal* one essentially overlap (Katsuo and Mazzotti 2010b; Katsuo et al. 2011). This is a very important result, on which the whole promise of the I-SMB process is based. The use of the optimizing controller offers the opportunity to demonstrate the same result in a different manner. Since the controller's objective function is defined in such a way to maximize productivity and minimize solvent consumption, the operating point towards which the controller converged should be very close to the tip of the *real* complete separation region derived as discussed above.

3.3 Application of the optimizing controller

In this section we finally present the results obtained by applying the I-SMB optimizing controller, and we compare them with those obtained when applying the optimizing SMB controller to the equivalent standard SMB processes. For the sake of brevity, we present here the results of eight simulations out of the many carried out to check the controller's performance, which consider the four implementations of the SMB and the I-SMB technologies considered at two different overall feed concentrations, namely 1 g/L and 15 g/L. These two feed concentration levels are representative of conditions close to linear chromatographic conditions and of concentration levels where nonlinear effects are very pronounced, respectively. It is worth noting that although the results presented here refer to the use of the controller when only the flow rates in Sects. 2 and 3 are manipulated, it is known from previous works that the controller performs well also when all four flow rates and the switch time are used as manipulating variables (Grossmann et al. 2009; Langel et al. 2010); it is however clear that modifying the switch time during operation would be particularly complex in the case of the I-SMB process where each switch period is subdivided in two subintervals.

The results are illustrated in terms of trajectory of the operating point within the (m_2,m_3) operating plane in Figs. 2 and 3, and in terms of evolution of product purities and productivity versus time in Figs. 4 and 5. Figures 2 and 4 refer to 1 g/L feed concentration, whereas Figs. 3 and 5 to 15 g/L.

In each of Figs. 2 and 3 two *ideal* complete separation regions are shown, namely the one seen by the virtual plant, i.e. calculated for the relevant feed concentration and plotted with solid boundaries, and the region seen by the controller, i.e. the linear right triangle with dotted boundaries. All controlled separations have been carried out with initially clean columns and from the initial operating point as given in Table 2 (upper left point in each figure, i.e. outside all complete separation regions). Note also that the controller has been activated only after a few cycles to show that indeed the product purities are spoiled in the initial operating point. The optimizing controller is expected to drive the operating conditions of the process towards the operating point in the operating space corresponding to optimal operating conditions, i.e. the tip of the *real* complete separation region. In fact, the detailed model used as virtual plant accounts for all the effects and physical mechanisms that are neglected by the Triangle Theory.

This is indeed what happens, as shown in Figs. 2 and 3. As expected, for the six column standard SMB process and for the six column and the four column I-SMB process (subfigures (a), (c) and (d) in each figure) the operating point reaches the tip of the *ideal* complete separation region, which as discussed above coincides with that of the *real* complete separation region, thanks to the action of the optimizing controller. On the contrary, for the four column standard SMB process (subfigure (b) in each figure) the operating point moves towards a point further inside the *ideal* complete separation region. Nevertheless the action of the controller is also in this case fully consistent with off-line optimization as discussed above in Sect. 2.

This result illustrates once more the advantage of the I-SMB process with respect to the standard SMB process. In essence, in a 1-1-1-1 SMB unit its sections are not fragmented enough to allow for an effective simulation of a countercurrent process, hence performance is penalized with respect to a 1-2-2-1 SMB process. This is not an issue any more in the I-SMB process, as we discussed in great

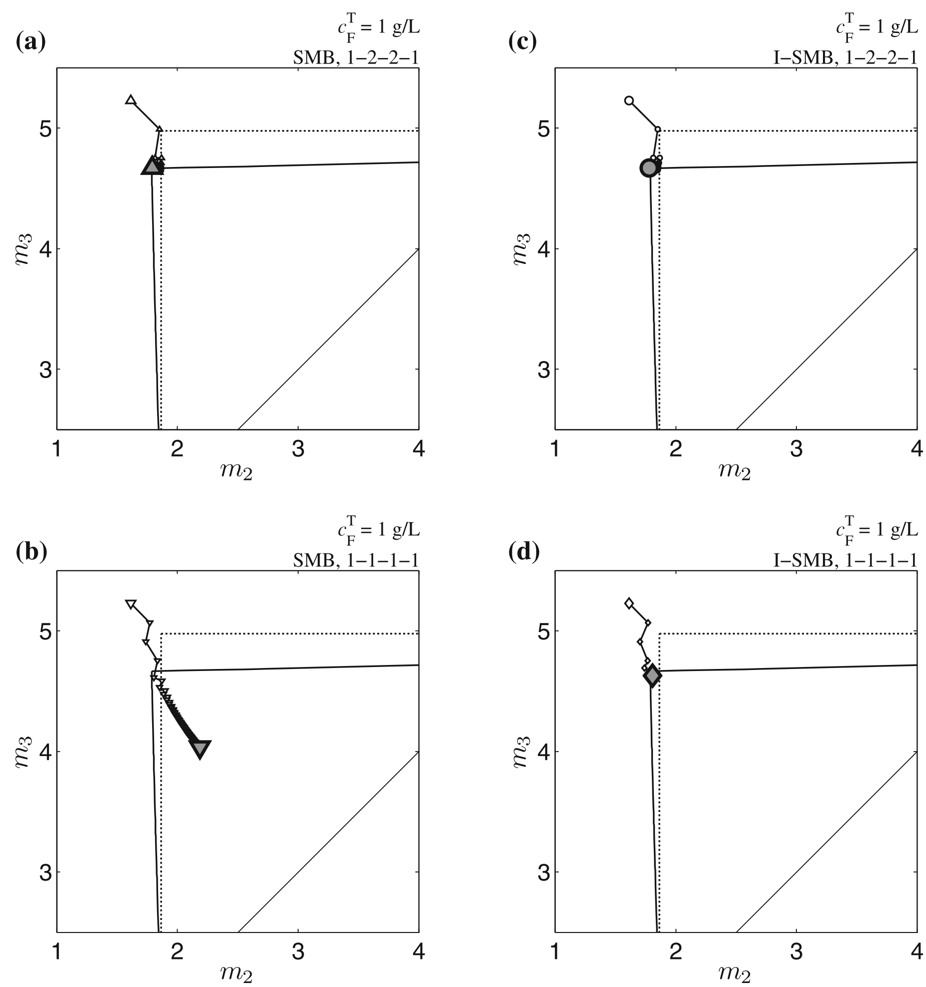

Fig. 2 Trajectory of operating points during the optimizing control of SMB/I-SMB process. Feed concentration: 1.0 g/L. **a** conventional SMB 1-2-2-1, **b** conventional SMB 1-1-1-1, **c** I-SMB 1-2-2-1, **d** I-SMB 1-1-1-1. *Grey colored symbol* final (m_2,m_3). *Solid line* complete separation region estimated with Bi-Langmuir isotherms, *dotted line*: *linear triangle*

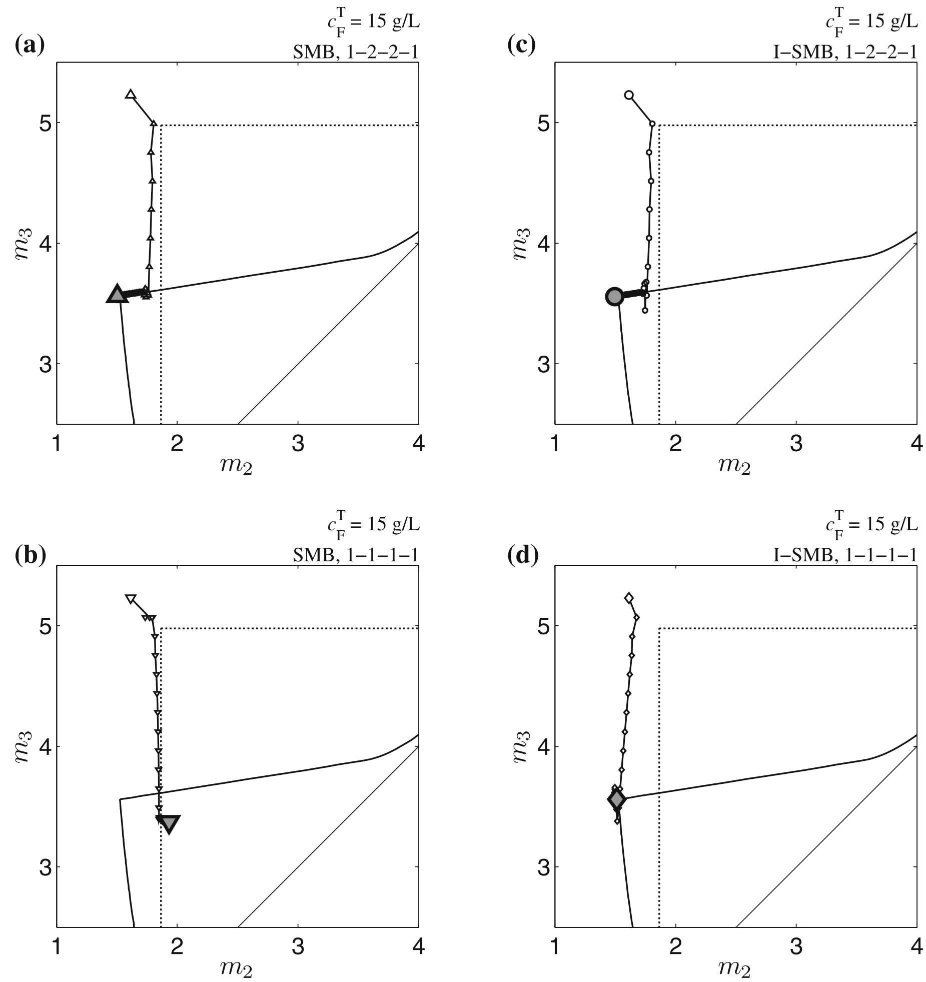

Fig. 3 Trajectory of operating points during the optimizing control of SMB/I-SMB process. Feed concentration: 15.0 g/L. **a** conventional SMB 1-2-2-1, **b** conventional SMB 1-1-1-1, **c** I-SMB 1-2-2-1, **d** I-SMB 1-1-1-1. *Grey colored symbol* final (m_2,m_3). *Solid line* complete separation region estimated with Bi-Langmuir isotherms, *dotted line*: *linear triangle*

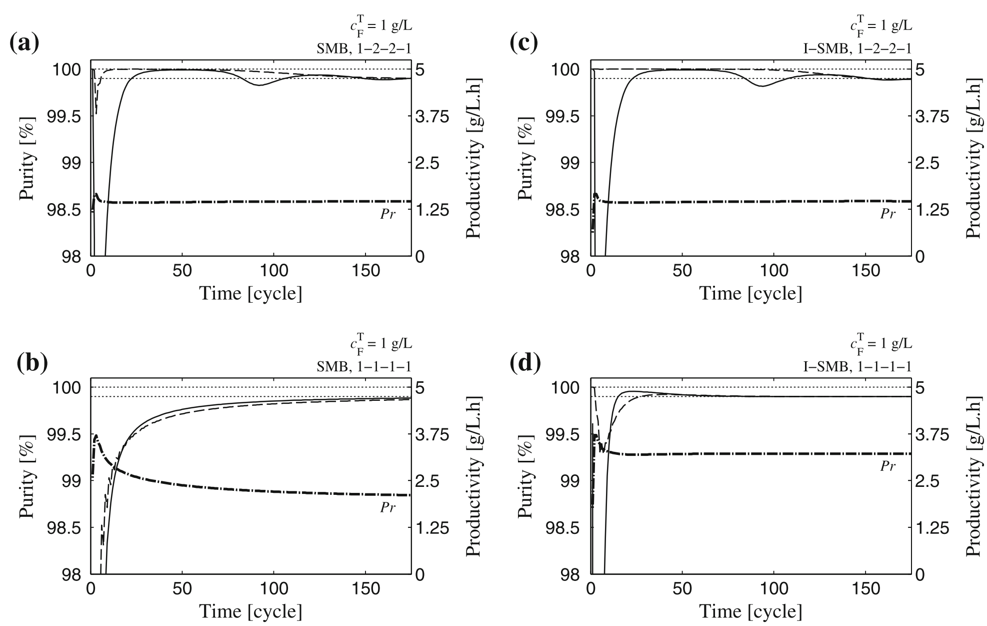

Fig. 4 Change of Extract and Raffinate product purities and productivity during the optimizing control of SMB/I-SMB process. Feed concentration: 1.0 g/L. **a** conventional SMB 1-2-2-1, **b** conventional SMB 1-1-1-1, **c** I-SMB 1-2-2-1, **d** I-SMB 1-1-1-1. *Solid line* Extract, *dashed line* Raffinate, *dotted line* products specification ($X_{A,\min}$, $X_{B,\min} = 0.999$), *dot-dashed thick line*: productivity (*Pr*)

detail earlier (Katsuo and Mazzotti 2010a) and further demonstrated in ensuing papers (Katsuo and Mazzotti 2010b; Katsuo et al. 2011).

Figures 4 and 5 present the same results from a different viewpoint. The most important information from these figures is that in all eight cases, i.e. four and six column

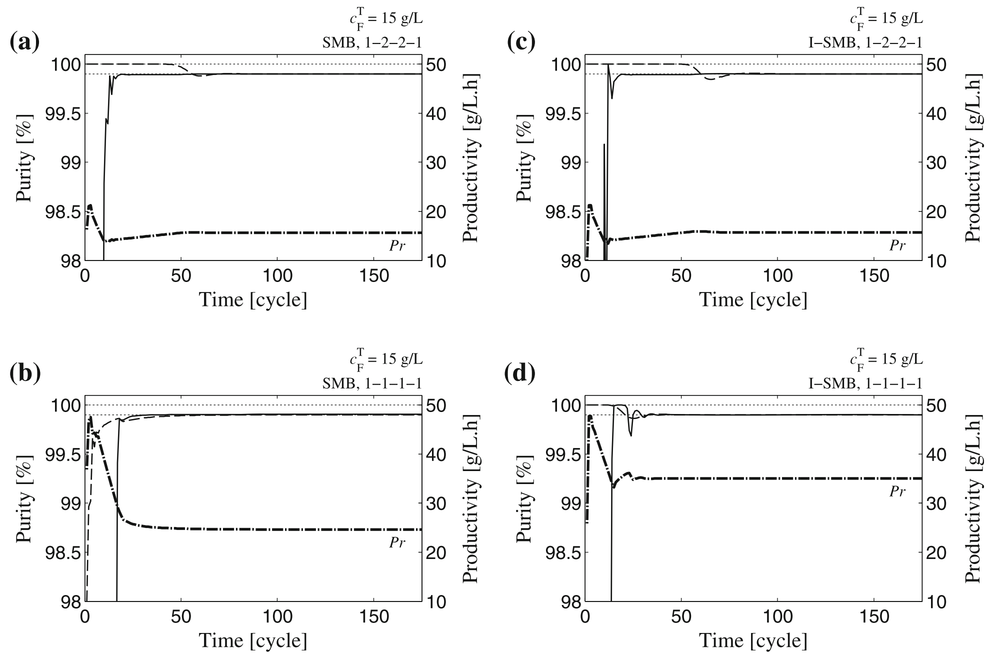

Fig. 5 Change of Extract and Raffinate product purities and productivity during the optimizing control of SMB/I-SMB process. Feed concentration: 15.0 g/L. **a** conventional SMB 1-2-2-1, **b** conventional SMB 1-1-1-1, **c** I-SMB 1-2-2-1, **d** I-SMB 1-1-1-1. *Solid line* Extract, *dashed line* Raffinate, *dotted line* products specification ($X_{A,min}$, $X_{B,min} = 0.999$), *dot-dashed thick line* productivity (*Pr*)

standard SMB and I-SMB at 1 and 15 g/L feed concentration, the required purity specifications of 99.9 % are fulfilled for both the extract (solid line) and the raffinate (dashed lines) products. In other words, in all cases the optimizing controller makes sure that the product specifications are fulfilled independent of productivity. It is worth noting that in the two figures, particularly in the case of the 1-2-2-1 SMB and I-SMB configurations, "undershoot" effects can be observed. Purities (both the extract and the raffinate purities in the case of Fig. 4, only the extract purity in Fig. 5) attain values better than the specification during the early cycles of the process. Then, operating conditions are adjusted to get closer to purity specifications, while improving in terms of objective function. In doing so, the controller dynamics, which is not tuned specifically for each different operating condition, drives the system out of specifications (between cycles 50 and 100, depending on the cases), before correcting and finally reaching the cyclic steady state.

At the same time however, it is also clear that the controller improves productivity and optimizes it (dot-dashed lines labeled *Pr* in the same figures). As one can see in Eqs. 19 and 20, the final value of the productivity depends on total feed concentration, on the final position of the operating parameters (m_2,m_3) and on the unit configuration, i.e. on the number of columns of the unit. For a given feed concentration, less columns and a larger value of the difference $m_3 - m_2$ yield higher productivity. In our cases, the productivity of the two six column processes is the same, whereas that of the two four column processes is always better than that of the six column processes. However, the 1-1-1-1 I-SMB reaches a productivity that is 40–50 % higher than the 1-1-1-1 standard SMB, since the latter can deliver the products in spec only for an operating point well inside the *ideal* complete separation region.

When comparing the productivity of the four column SMB and I-SMB processes to that of the equivalent six column processes a note of warning is necessary. In this work, for the sake of the simplicity in the use of the controller, we have kept switch time, flow rate ratios m_1 and m_4 and, most importantly, column length constant. The results obtained here are of course valid under these assumptions. If not only the operating conditions but also column size and switch time were optimized for all four processes independently, one would obtain different column sizes for the different processes and the results in terms of productivity might be less different for four column and six column processes.

The analysis and results presented here prove that the optimizing controller developed and applied to the standard SMB process is able to control and optimize the I-SMB operation as well, even where the mixture to be separated is clearly subject to a nonlinear adsorption isotherm and the feed concentration is larger. While reconfirming the favorable and promising characteristics of the I-SMB process in a four-column 1-1-1-1 configuration, i.e that the same purity levels can be attained at very similar operating conditions as in a 1-2-2-1 configuration but with less columns, the use of the optimizing controller in the I-SMB process promises to offer even more opportunities to exploit its superior economic potential.

References

Abel, S., Erdem, G., Mazzotti, M., Morari, M., Morbidelli, M.: Optimizing control of simulated moving beds—linear isotherm. J. Chromatogr. A **1033**, 229 (2004)

Amanullah, M., Grossmann, C., Mazzotti, M., Morari, M., Morbidelli, M.: Experimental implementation of automatic 'cycle to cycle' control of a chiral simulated moving bed separation. J. Chromatogr. A **1165**, 100 (2007)

Erdem, G., Abel, S., Morari, M., Mazzotti, M., Morbidelli, M., Lee, J.H.: Automatic control of simulated moving beds. Ind. Eng. Chem. Res. **43**, 405 (2004)

Erdem, G., Abel, S., Morari, M., Mazzotti, M., Morbidelli, M.: Automatic control of simulated moving beds-II: nonlinear isotherm. Ind. Eng. Chem. Res. **43**, 3895 (2004)

Gentilini, A., Migliorini, C., Mazzotti, M., Morbidelli, M.: Experimental implementation of automatic 'cycle to cycle' control to a nonlinear chiral simulated moving bed separation. J. Chromatogr. A **805**, 37 (1998)

Grossmann, C., Amanullah, M., Morari, M., Mazzotti, M., Morbidelli, M.: Optimizing control of simulated moving bed separations of mixtures subject to the generalized Langmuir isotherm. Adsorption **14**, 423 (2008)

Grossmann, C., Amanullah, M., Erdem, G., Mazzotti, M., Morbidelli, M., Morari, M.: 'Cycle to cycle' optimizing control of simulated moving beds. AIChE J. **54**, 194 (2008)

Grossmann, C.: Optimizing model predictive control of multi-column chromatographic processes. PhD Dissertation, ETH Zurich (2009)

Grossmann, C., Langel, C., Mazzotti, M., Morari, M., Morbidelli, M.: Experimental implementation of automatic 'cycle to cycle' control to a nonlinear chiral simulated moving bed separation. J. Chromatogr. A **1217**, 2013 (2010)

Katsuo, S., Mazzotti, M.: Intermittent simulated moving bed chromatography: 1. Design criteria and cyclic steady-state. J. Chromatogr. A **1217**, 1354 (2010)

Katsuo, S., Mazzotti, M.: Intermittent simulated moving bed chromatography: 2. Separation of Tröger's base enantiomers. J Chromatogr. A **1217**, 3067 (2010)

Katsuo, S., Langel, C., Sandré, A.-L., Mazzotti, M.: Intermittent simulated moving bed chromatography: 3. Separation of Tröger's base enantiomers under nonlinear conditions. J. Chromatogr. A **1218**, 9345 (2011)

Kessler, L.C., Seidel-Morgenstern, A.: Improving performance of simulated moving bed chromatography by fractionation and feed-back of outlet streams. J. Chromatogr. A **1207**, 55 (2008)

Langel, C., Grossmann, C., Morbidelli, M., Morari, M., Mazzotti, M.: Implementation of an automated on-line high-performance liquid chromatography monitoring system for 'cycle-to-cycle' control of simulated moving beds. J. Chromatogr. A **1216**, 8806 (2009)

Langel, C., Grossmann, C., Jermann, S., Mazzotti, M., Morari, M., Morbidelli, M.: Experimental optimizing control of the simulated moving bed separation of Tröger's base enantiomers. Ind. Eng. Chem. Res. **49**, 11996 (2010)

Ludemann-Hombourger, O., Nicoud, R.M., Bailly, M.: The "VARICOL" process: a new multicolumn continuous chromatographic process. Sep. Sci. Technol. **35**, 1829 (2000)

Mazzotti, M.: Equilibrium theory based design of simulated moving bed processes for a generalized Langmuir isotherm. J. Chromatogr. A **1126**, 311 (2006)

Mazzotti, M., Storti, G., Morbidelli, M.: Optimal operation of SMB units for nonlinear chromatographic separations. J. Chromatogr. A **769**, 3 (1997)

Rajendran, A., Paredes, G., Mazzotti, M.: Simulated moving bed chromatography for the separation of enantiomers. J. Chromatogr. A **1216**, 709 (2009)

Schramm, H., Kienle, A., Kaspereit, M., Seidel-Morgenstern, A.: Improved operation of simulated moving bed processes through cyclic modulation of feed flow and feed concentration. Chem. Eng. Sci. **58**, 5217 (2003)

Sturm, J.F.: Using SeDuMi 1.02, a Matlab toolbox for optimization over symmetric cones. Optim. Method. Softw. **11–12**, 625 (1999)

Zhang, Z., Mazzotti, M., Morbidelli, M.: PowerFeed operation of simulated moving bed units: changing flow-rates during the switching interval. J. Chromatogr. A **1006**, 87 (2003)